Carbonates and Evaporites (2019) 34:115–132
https://doi.org/10.1007/s13146-018-0449-7

ORIGINAL ARTICLE

Petrography and geochemical constrain on dolostones of the Shahbazan Formation in Lorestan (Iran)

Morteza Hassanzadeh Nemati[1] · Hassan Mohseni[1] · Mahmoud Memariani[2] · BizhanYousefi Yeganeh[3] · Mohadeseh Janbaz[1] · Rudy Swennen[4]

Accepted: 25 March 2018 / Published online: 22 May 2018

Abstract

The Shahbazan Formation (Fm.) was deposited in the Lorestan subzone of the Zagros Basin during middle to late Eocene, which presently is part of the Zagros fold and thrust belt. The Shahbazan Fm. consists of limestone and dolostone beds, which hosts some considerable hydrocarbon occurrences in the Zagros basin. In the present study, the reference Mamulan and Murani sections in the Lorestan province were studied. A total of 330 samples were collected. Petrographic examination of stained sections (alizarin red S and potassium ferricyanide) allowed differentiating five types of dolomites within the Shahbazan Fm. Within the Mamulan section, three distinct types where defined including dolomicrite (D1), associated by evaporites, peloides, intraclast, and algal laminites; dolomicrosparite (D2), with well-preserved algal laminites; and limpid dolosparite (D3) locally embedded within poikilotopic anhydrite. The Murani section comprises fabric-destructive dolosparite (D4), pore-filling dolomite (D5), as well as D1. Some fractures of the Shahbazan Fm. were occluded by evaporites and calcite spars in the Mamulan and Murani sections, respectively. The pore-filling (D5) dolomite displays a fine zonation pattern under CL, which may reflect successive growth stages during shallow to relatively burial diagenesis. According to microfacies analysis, seven microfacies including dolomudstone (F1), dolomitized bioclast–intraclast wackestone to packstone (F2), dolomitized lime mudstone (F3), interbedded laminated lime mudstone and evaporites (F4); dolomitized peloid packstone to wackestone (F5); dolomitized intraclast bioturbated wackestone (F6); bioclast miliolid wackestone to packstone (F7), as well as various anhydrites (e.g., nodular and laminated) were recognized which suggest intertidal–supratidal depositional setting for the Shahbazan Formation. ICP-MS analysis on some selected samples of the D1, revealed their chemical composition with an average for Fe of 1291 and 185 ppm, for Na of 644 and 650 ppm, for Sr of 125 and 185 ppm, and a Mg/Ca ratio of 0.57 and 0.505, for Mn of 23 ppm (only for Mamulan section) in the Mamulan and Murani sections, respectively. Relatively high Mg/Ca ratio suggests that these dolomites might be originated from salt waters. The Sr/Ca vs Mn suggests a relatively semi-closed diagenetic system. Variable Fe and Mn contents are probably due to reaction with meteoric water.

Keywords Shahbazan Fm. · Dolomite petrography · Geochemistry · Zagros basin · Iran

✉ Hassan Mohseni
mohseni@basu.ac.ir

Morteza Hassanzadeh Nemati
mhn198648@yahoo.com

Mahmoud Memariani
memarianim@gmail.com

BizhanYousefi Yeganeh
bizhan.yegane@gmail.com

Mohadeseh Janbaz
mjanbaz90@basu.ac.ir

Rudy Swennen
rudy.swennen@kuleuven.be

[1] Department of Geology, Faculty of Science, Bu-Ali Sina University, Hamedan, Iran

[2] Geosciences Division, Research Institute of Petroleum Industry (RIPI), Tehran, Iran

[3] Department of Geology, Faculty of Science, University of Lorestan, Khorramabad, Iran

[4] Earth and Environmental Sciences, KU Leuven, Louvain, Belgium

Introduction

Dolomitization often vitally affects porosity in carbonate reservoirs. This process may affect limestone beds where a considerable amount of diagenetic fluids with variable temperature and chemical composition percolate through them (Warren 2000; Machel 2000). Replacive dolomitization and pore-filling dolomites often control porosity development during diagenetic history of carbonate rocks (Azomani et al. 2013). The Shahbazan Fm. and its lateral equivalents host considerable amount of hydrocarbon in the Zagros Basin (Motiei 1995; Mohseni et al. 2016). Consequently, unraveling the dolomitization history of the Shahbazan Fm. and its effect on porosity development are of major interest. The Shahbazan Fm. was deposited during the middle to late Eocene (James and Wynd 1965; Motiei 1995; Alavi 2004) as a carbonate-dominated interval overlying the clastic rocks of the Kashkan Fm. and disconformably underlying by the carbonates of the Asmari Fm. However, the Shahbazan Fm. passes laterally into fine-grained shale and mudstone-dominated intervals of the Pabdeh Fm. toward the distal part of the Zagros basin. Eastern ward of the Zagros basin passes into the dolostones of the Jahrum Fm., which in turn hosts some hydrocarbon reserves (James and Wynd 1965; Motiei

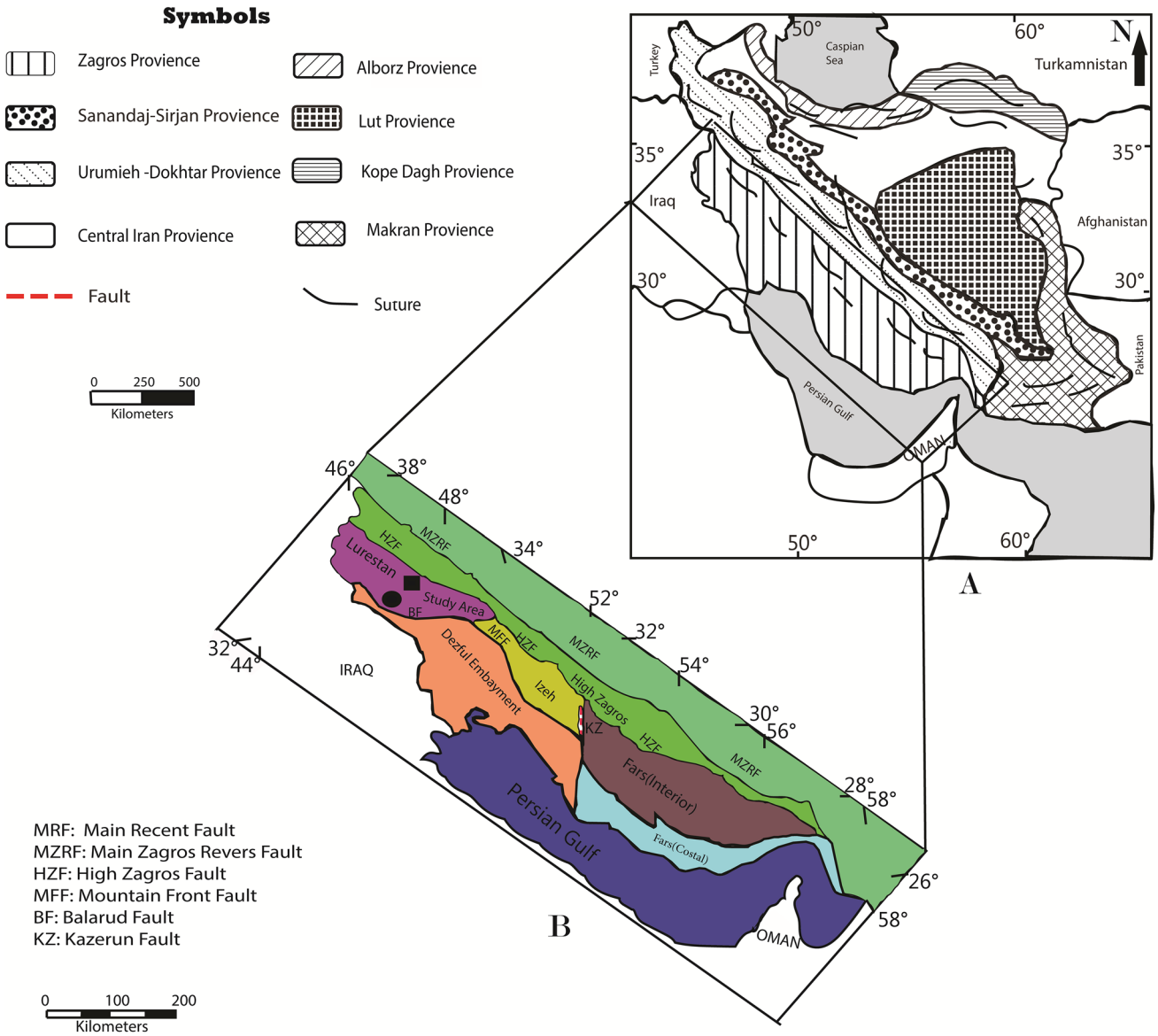

Fig. 1 **a** Main tectono-sedimentary basins of Iran, after Heydari (2008). **b** Simplified geology map of the Lorestan subzone, after Motiei (1995); studied sections are marked by solid square and circle

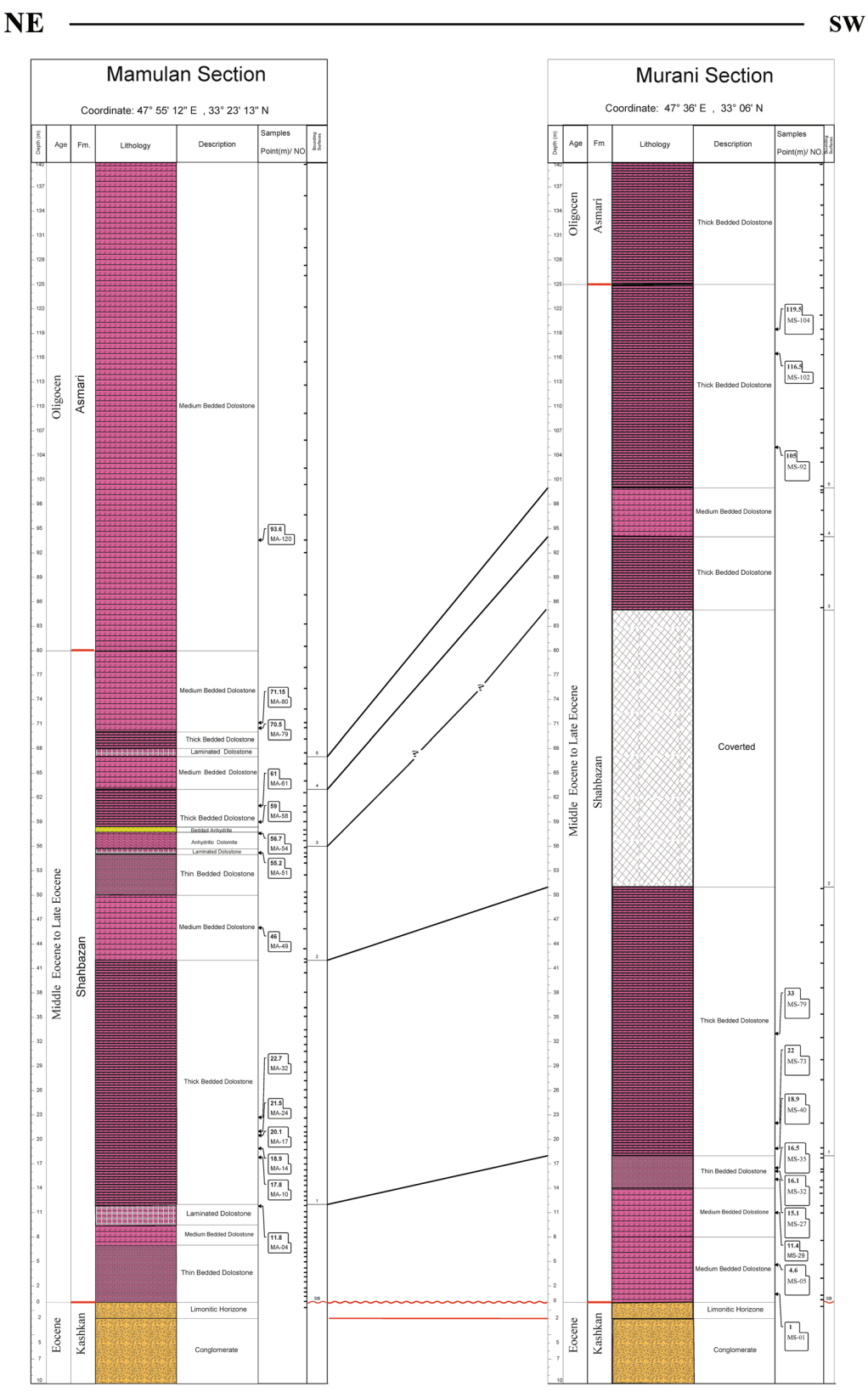

Fig. 2 Stratigraphic log of the Shahbazan Formation in the Mamulan section (right) and Murani section (left). Thickness in meter

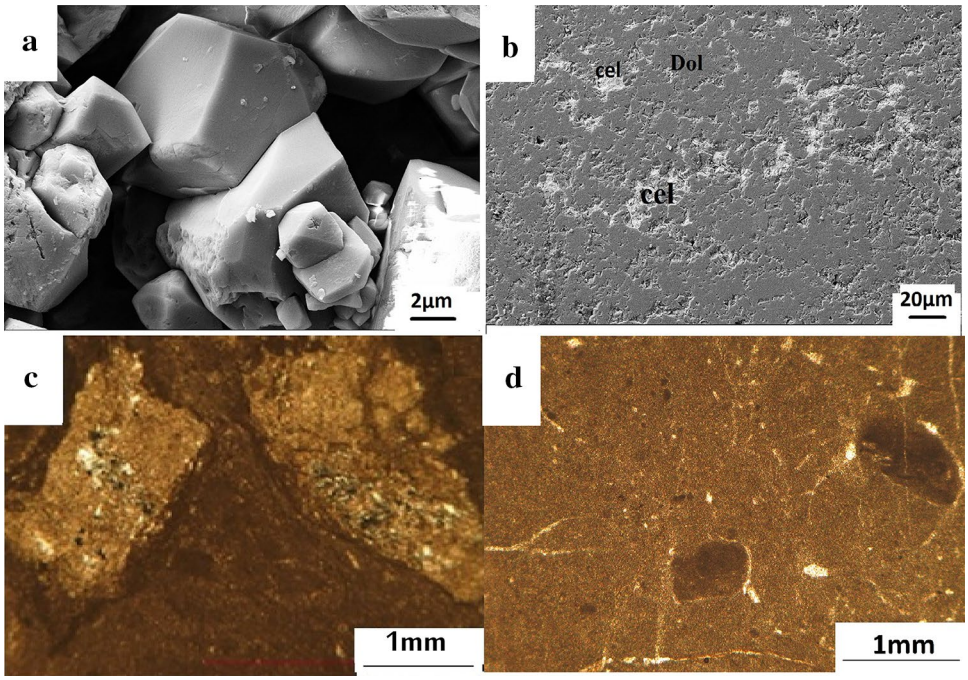

Fig. 3 **a** SEM photo of dolomicrites (D1) of the Shahbazan Fm. in the Mamulan section. Note intercrystalline porosity between dolomite rhombs. **b** Backscattered SEM photograph of D1 and evaporitic minerals (celestite), **c**, **d** intraclast and mud crakes accompanying D1, which imply upper intertidal to supratidal setting (Mamulan section, PPL)

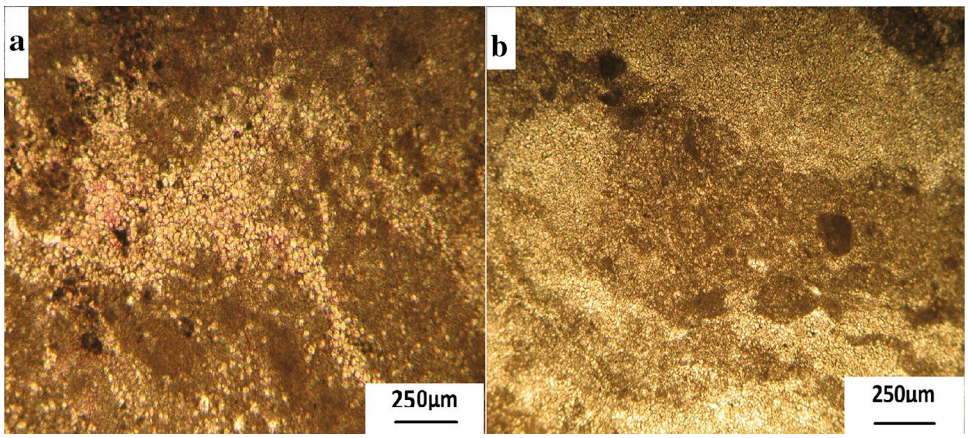

Fig. 4 **a**, **b** Photomicrograph of D1 with remnants (ghost) of algal laminites (Mamulan section, PPL)

1995, Alavi 2004). The Shahbazan Fm. shows extensive dolomitization in the majority of the Zagros Basin (Mohseni et al. 2012), particularly in the Lorestan subzone (a subdivision of the Zagros Basin), where the two sections selected for this study are located (Fig. 1a, b).

Methods and materials

Two surface sections of the Shahbazan Fm. named Mamulan and Murani were samples in the Lorestan province (Fig. 1a) for petrographic and geochemical examinations on dolomites. The Shahbazan Fm. is about 80 m and 125 m thick in the Mamulan and Murani sections, respectively (Fig. 2). A total of 330 samples were collected (average sampling interval of 0.5 m). The thin sections prepared from hand specimens were stained by alizarin red S and potassium ferricyanide (Dickson 1965). Furthermore, five selected thin polished samples were examined under CL microscope model MK4 CCL 8200 at 15 kV and 400 mA condition at the RIPI (Research Institute for Petroleum Industry, Tehran). A suite of five selected samples was also analyzed by SEM (model Zeiss-ΣIGMA/VP) at the Applied Research Centre of the Geological Survey of Iran (Karaj City). Simultaneous semi-quantitative analysis was performed to reveal the chemical composition of the dolomite crystals by EDX (model X-MAX). Fifteen selected

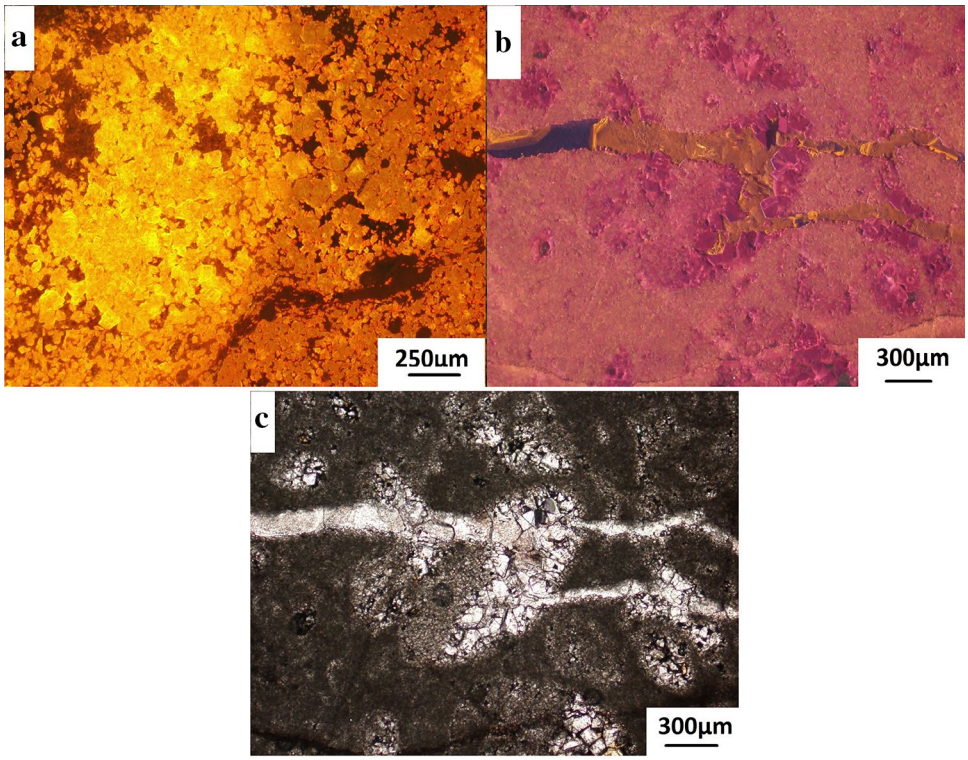

Fig. 5 **a** Algal laminite under CL, bright luminescence is caused by organic matter. **b** CL photo of a packstone in which the grains are cut by fractures during telogenesis. **c** Same as **b** under PPL, Murani section

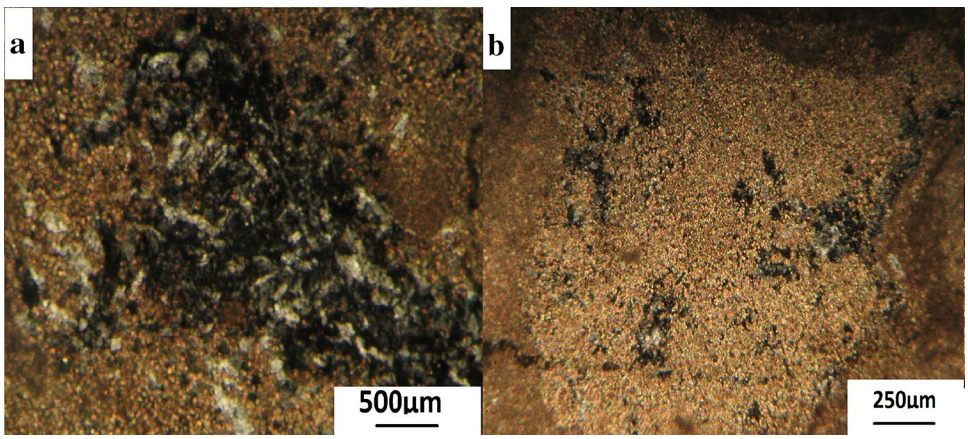

Fig. 6 Photomicrographs of clear dolomite (D3). **a**, **b** The dolomite crystals embedded in evaporative minerals, XPL, Mamulan section

samples of dolomicrites (D1) were also analyzed with ICP-MS (model Agilent Series 4500 HP at Zar Azma Mineral Studies Company, Iran. Rst. was > 97%, $R^2 > 0.99$). Electron probe microanalysis (EPMA) by JEOL JXA-8530F instrument was done on scattered dolomite crystals to get information about their composition. The accelerating voltage was 15 kV, with a probe current of approximately 10–0.5 µA at the Department of Earth and Environmental Sciences of the KU Leuven (Belgium). Textural and crystal description of dolomites was after Sibley and Gregg (1987). Petrography and textural description of limestone was after Dunham (1962).

Geological setting

The study area (Lorestan subzone) is a part of the Zagros fold and thrust belt (Fig. 1b) (Stocklin 1968; Heydari 2008). This part of the basin is characterized by continuous sedimentation during late Permian to Miocene, with predominant carbonate and subordinate evaporite and clastic deposition (Murris 1980; Motiei 1995; Sepehr and Cosgrove 2004;

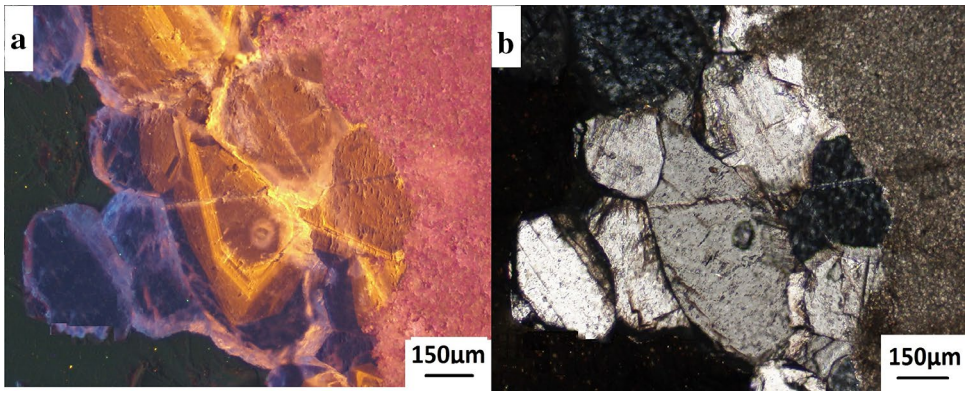

Fig. 7 **a**, **b** CL and photomicrograph of the pore-filling spar and possibly a sulfide mineral? (see also Fig. 13), Murani section, **b** under PPL

Alavi 2007). These successions are well exposed in the Lorestan subzone, particularly those of Cretaceous onward. Some formations of these successions are well appreciated as the part of petroleum play of the Zagros Basin (Razin et al. 2010). However, the Shahbazan Fm., which is partially dolomitized, has being less studied, despite it hosts some hydrocarbons in the Zagros Basin. However, its lateral equivalent, the Pabdeh Fm. was subject of considerable studies as it is considered as an effective source rock (Ala et al. 1980; Ala 1982; Bordenave and Burwood 1990; Mohseni and Al-Aasm 2004; Mohseni et al. 2011).

Results

Petrography of dolomites

Based on petrographic examination of thin sections, five distinct dolomite types were recognized within the Shahbazan Fm. designated as D1 through D5, namely.

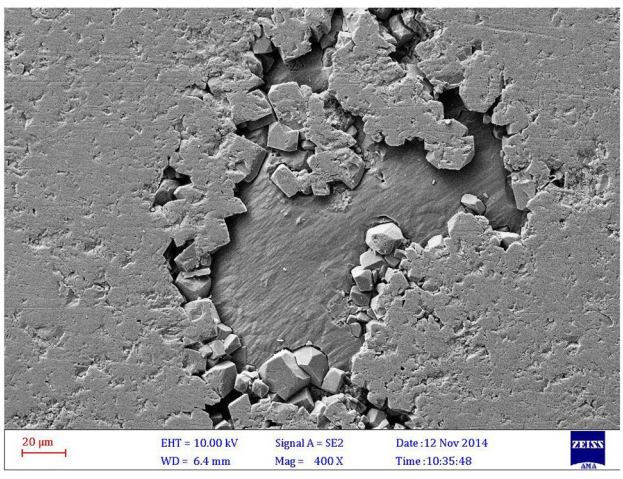

Fig. 8 SEM photo of pore lining D4 dolomite in the moldic porosity; D4 was only observed in Murani section

D1 (dolomicrite)

This very finely crystalline dolomite is the most prominent dolomite type, as it comprises about 85% of dolostones of the Shahbazan Fm. in the study area. These crystals are anhedral with less than 4 µm (exceptionally up to 16 µm) crystal size; D1 is similar to xenotopic dolomicrites described by Friedman (1965), the xenotopic-A of Gregg and Sibley (1984), or the non-planar texture of Sibley and Gregg (1987) as well as the non-planar anhedral of Mazzullo (1992). D1 is associated with primary sedimentary structures including lamination, fenestral fabric along with intraclast, peloids, and rare bioclasts (Fig. 3).

D2 (dolomicrosparite)

The crystal size varies between 16 and 60 µm with anhedral to subhedral crystals with straight boundaries which comprises 4% of the dolostones. However, in dolomicrosparite with preserved algal lamanites, their size varies between 25 and 50 µm (Fig. 4). D2 is similar to the idiotopic texture of Friedman (1965), the idiotopic of Gregg and Sibley (1984), or the planar-porphyrotopic dolomite described by Mazzullo (1992). Bright luminescence of algal laminite under CL is caused by organic matter and packstone, in which the grains are cut by fractures during tellogenesis (Fig. 5).

D3 (limpid dolomite)

D3 was observed exclusively in the uppermost part of the Shahbazan Fm. in the Mamulan section (top 45 m) with about 3% frequency. They are inclusion-free euhedral crystals with average 25 µm size and visible zoning. Clear limpid dolomite crystals are embedded within porphyrotopic anhydrite (Fig. 6).

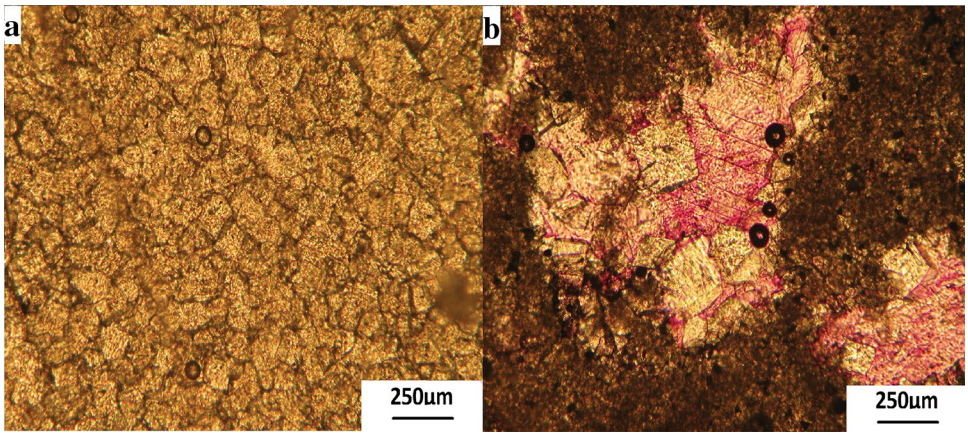

Fig. 9 **a** Photomicrograph of dolosparite with curved crystal boundaries (PPL); **b** Dolomite crystals in vuggy pores (up to 250 µm) embedded in calcite matrix, XPL, stained thin section; Shahbazan Fm., Murani section

D4 (pore-filling dolosparite)

Crystal size varies between 100 and 400 µm depending on available pore space. Euhedral dolomite crystals preferentially line up along former pore spaces as well as moldic porosity (sensu Choquette and Pray 1970) (Figs. 7, 8). D4 is similar to idiotopic texture of Friedman (1965), the idiotopic-A dolomites of Gregg and Sibley (1984), the planar texture of Sibley and Gregg (1987), or the pore-filling planar texture of Mazzullo (1992). This type of dolomite comprises 3% of the total dolostones and is associated with sulfide minerals (Fig. 7).

D5 (dolosparite)

anhedral crystal with curved and/or irregular boundaries varies between 70 and 250 µm in size. This type comprises 5% of the dolostones. However, some subhedral crystals with straight boundaries (compromise boundary?) were also observed (Fig. 9a). This type is similar to the hypidiotopic-s

Table 1 Summarized data of microfacies of the Shahbazan samples studied in Mamulan and Murani sections

Microfacies code	Microfacies name	Main lithology	Main allochems	Minor allochems	Sedimentary structures and porosity	Sections which has been detect	Interpretation
F1	Dolomudstone	Dolostone	Intraclast (20%)	Peloid (5%)	Lamination, fenestral fabric along with intraclast, fracture, vuggy porosity	In both sections	Supratidal
F2	Dolomitized bioclast–intraclast wackestone to packstone	Limestone	Intraclast (30%), Benthic foram. (10–15%)	Echinoid (3%); bivalve (2%); gastropoda (2%)	Bioturbation, moldic porosity	Seems in both sections but in Mamulan section is dominated	Supratidal
F3	Dolomitized lime mudstone	Limestone, anhydrite (5%)	–	Ostracoda. (3%)	Vuggy and moldic porosity	Mamulan	Supratidal
F4	Lamination evaporite–carbonate mudstone	Limestone, anhydrite	–	–	Lamination, vuggy porosity	Mamulan	Sabkha
F5	Dolomitized peloid packstone to wackestone	Limestone	Peloid (35%)	Intraclast (5%)	Bioturbation, algal laminite	In both sections	Intertidal
F6	Dolomitized intraclast bioturbated wackestone	Anhydrite	Intraclast (40%)	Bioclast (2–3%)	Bioturbation	Mamulan	Intertidal
F7	Bioclast miliolid wackestone to packstone	Limestone	Benthic foram (miliolid; 30%). Ostracoda (10%)	Echinoid (3–4%); bivalve (2%)	Rarely porosity	In both sections	Lagoonal

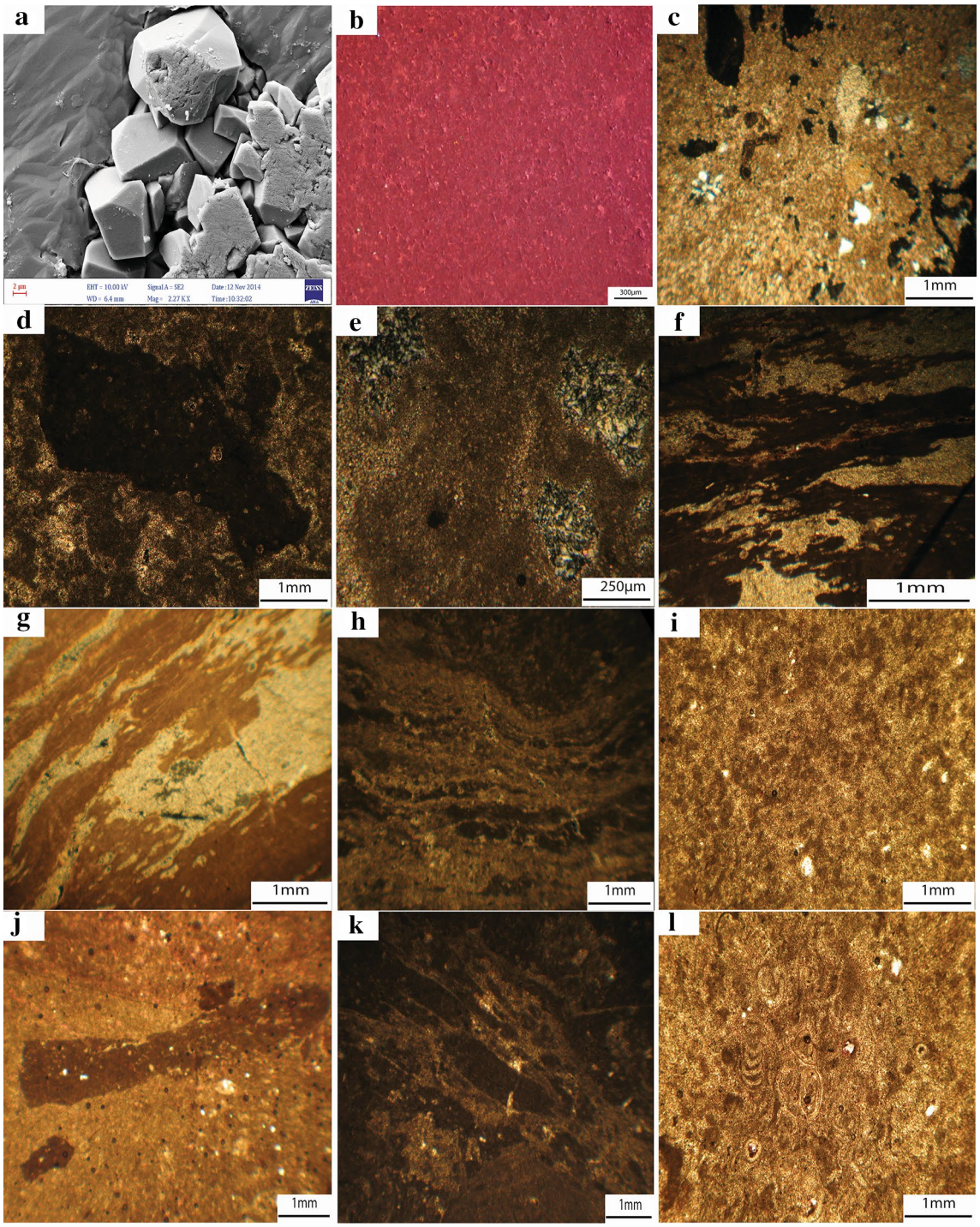

Fig. 10 Microfacies types of the Shahbazan Formation. F1 (dolomudstone). **a** SEM photograph of xenotopic to idiotopic subhedral to euhedral dolomite, Murani section. **b** The same texture under CL. **c** Example of F1, XPL, Mamulan section. **d** F2 (dolomitized intraclast wackestone) XPL, Mamulan section. **e**, **f** F3 (dolomitized lime mudstone) associated with evaporative minerals and fenestral fabric, XPL, Mamulan section. **g**, **h** F4 [laminated evaporite (anhydrite)–carbonate mudstone]; PPL and XPL, respectively, Mmulan section. **i** F5 (dolomitized peloid packstone to wackestone), PPL, Murani section. **j**, **k** F6 (dolomitized falt-pebble bioturbated intraclast wackestone–packstone), PPL, Mamulan section, Murani section, XPL, respectively. **l** F7 (bioclast miliolid wackestone to packstone), Mamulan section, PPL

texture of Friedman (1965), the idiotopic of Gregg and Sibley (1984), or the planar, subhedral texture of Sibley and Gregg (1987) and Mazzullo (1992). D5 is fabric destructive (Fig. 9b), obliterating the primary sedimentary structures.

Microfacies characteristics

Petrographic examinations on thin sections including existing allochemical and orthochemical components and textural characteristics revealed that the Shahbazan Formation comprises seven microfacies in the Mamulan and Murani sections including: (F1): dolomudstone; (F2): dolomitized bioclast–intraclast wackestone to packstone; (F3): dolomitized lime mudstone; (F4): laminated evaporite–carbonate mudstone; (F5): dolomitized peloid packstone to wackestone; (F6): dolomitized intraclast bioturbated wackestone; and (F7): bioclast miliolid wackestone to packstone, which are summarized in Table 1 These microfacies will be briefly discussed in the following section.

F1 (dolomudstone)

This microfacies includes xenotopic to idiotopic subhedral to euhedral dolomite with dolomitized intraclast (20%), algal laminite (10%), and 5% peloids (Fig. 10a–c).

F2 (dolomitized bioclast–intraclast wackestone to packstone): this microfacies consists of intraclast, benthonic foraminifers (i.e., milliolid), ostracod, gastropod, and rare echinoderm fragments (Fig. 10d).

F3 (dolomitized lime mudstone)

This microfacies contains rare fossil fragments (occasionally ostracod), with 15% evaporative minerals (gypsum and anhydrite, only in the Mamulan section) and fenestral fabric (Fig. 10e, f).

F4 (laminated evaporite–carbonate mudstone)

This is basically barren and/or contains rare fossil fragments. Laminated to massive anhydrite may imply a sabkha-type environment. These beds are only limited to the lowermost 40 m part of the Mamulan section. Lack of biota and evaporite minerals suggest a restricted saline conditions in upper intertidal (Fig. 10g, h).

F5 (dolomitized peloid packstone to wackestone): This microfacies contains 30–40% peloids, few intraclast (5%), with remnants of algal laminae and collated fabric as well, which was interpreted as a peritidal (upper intertidal) facies (Fig. 10i).

F6 (dolomitized intraclast bioturbated wackestone)

Intraclast are the main constituent of this facies (40%) that rest on a mud matrix which imply intermittent exposure of the sediments. Hence, an intertidal setting is more plausible for this microfacies. Few pellet and bioclastic fragments are also present (Fig. 10j, k).

F7 (bioclast miliolid wackestone to packstone)

About 30–40% bioclasts including miliolid and ostracods are the main biota of this microfacies which suggest a lagoonal setting (Fig. 10l).

Table 2 Results of ICP-MS analysis of some elements of the D1 dolomite from Mamulan and Murani sections

Sample no.	Mg%	Ca %	Sr (ppm)	Fe (ppm)	Na (ppm)	Mn (ppm)
MA-04	12.56	21.47	116.9	2337	658	102
MA-14	12.47	21.31	195.7	1045	631	13
MA-17	12.76	22.11	94.9	710	620	9
MA-24	12.65	22.42	102.5	1125	671	6
MA-32	12.93	23.04	135.6	168	635	3
MA-49	12.87	22.81	127	612	632	4
MA-58	12.28	20.79	221.5	2794	559	58
MA-61	12.42	22.08	95.7	1157	582	29
MA-79	12.17	22.92	82.2	1722	739	4
MA-80	12.58	22.22	76.9	1246	715	3
MA-05	12.77	22.47	124.1	1226	645	–
MA-32	12.76	23.14	380.3	300	638	–
MA-35	12.77	22.57	140.9	348	605	–
MA-40	13.33	23.4	196.4	476	662	–
MA-73	12.81	22.45	86.9	558	702	–

Table 3 Results of Microprobe analysis of dolomite and evaporites from Murani to Mamulan sections

Sample no.	Spectrum	Petrography	MgO (wt%)	Mg (wt%)	Ca (wT%)	Sr (wT%)	S (wt%)	CaO (wt%)	SiO_2 (wt%)	Si (wt%)	O (wt%)	SrO (wt%)
MA117-a	1	Evaporite	–	–	28.05	–	23.49	63.32	–	50.11	49.89	–
	2	Silica	–	–	–	–	–	–	100	24.93	57.74	–
	3	Evaporite	–	–	27.96	–	23.81	62.94	–	44.57	55.43	–
MA117-b	1	Celestite	–	–	–	45.9	26.78	–	–	–	35.99	73.22
	2	Evaporite	–	–	32.69	–	17.33	63.72	–	–	40.65	–
MS103-d	1	Dolomite	43.32	17.17	25.28	–	–	56.68	–	–	57.55	–
	2	Calcite cement	–	–	49.78	–	–	100	–	–	50.22	–
	3	Dolomite	42.70	17.35	26.30	–	–	57.30	–	–	56.35	–
	4	Dolomite	41.82	17.54	27.67	–	–	58.18	–	–	54.79	–
	5	Calcite cement	–	–	49.63	–	–	100	–	–	50.37	–
MS103-c	1	Dolomite	41.77	17.17	27.09	–	–	58.23	–	–	55.74	–
	2	Calcite cement	–	–	50.38	–	–	100	–	–	49.62	–
	3	Dolomite	42.61	19.13	29.41	–	–	57.39	–	–	51.45	–
	4	Calcite cement	–	–	48.33	–	–	100	–	–	51.67	–

Interpretation

The microfacies types in the both sections suggest they were deposited in sabkha, upper intertidal to tidal flat in the Mamulan section, whereas intertidal to lagoon condition was more prevailed in the Murani section. Evidences such as exclusive deposition of evaporite minerals in the Mamulan section decrease in non-skeletal components and more frequent, and divers biota in the Murani section obviously reveal a proximal to distal proxy from the Mamulan section toward the Murani section in the study area.

Geochemistry of dolomites

Only D1 is frequent (about 85%) and the other types are very rare, intimately mixed, and interlocking on thin sections. Hence, to avoid any possible mixing of different dolomite types, we had only one choice to focus our geochemical studies on the D1. In other words, it was almost impossible to obtain separate pure samples of the other dolomite types avoiding any possible contamination due to phase mixing. Results of ICP-MS analysis of 15 selected samples of dolomicrites (D1) (10 samples from Mamulan section and 5 samples dedicated to Murani section) are presented in Table 2. In addition, some dolomite and evaporite samples were analyzed by microprobe (Table 3).

Ca and Mg

Average Ca content is 22.11 and 22.8% and for Mg 12.56% and 12.8% of the samples taken from Mamulan to Murani sections, respectively. Their Mg/Ca ratio (wt%) is 0.57 0.565 as well. Evidences support that D1 was deposited on peritidal setting, where storm events in upper tidal flat and consequent evaporation, and promotes precipitation of evaporites, which could rise the Mg^{2+}/Ca^{2+} ratio of fluids. The Mg-enriched fluids may promote dolomitization of limestones (McKenzie et al. 1980). Although the Mg/Ca ratio of fluids and stoichiometry of dolomites are not interdependent (Kaczmarek and Sibley 2011). However, concentration of major elements (e.g., Ca and Mg) in dolomites depends on Mg^{2+}/Ca^{2+} of dolomitizing fluids (Sass and Bein 1988). Percolation of Mg^{2+}-rich fluids could increase the Mg^{2+}/Ca^{2+} ratio of dolomites (Figs. 11, 12).

Dolomicrites are normally more frequent than other dolomite types (Azmy et al. 2009). Depositional feature (see above) and their finely crystalline texture suggest that these dolomites are formed in low temperature, at near surface condition. Similar features are well accepted for early penecontemporaneous dolomites formed in supratidal to intertidal settings (Al-Aasm and Packard 2000; Warren 2000; Lasemi et al. 2012; Haeri Ardakani et al. 2013). They were

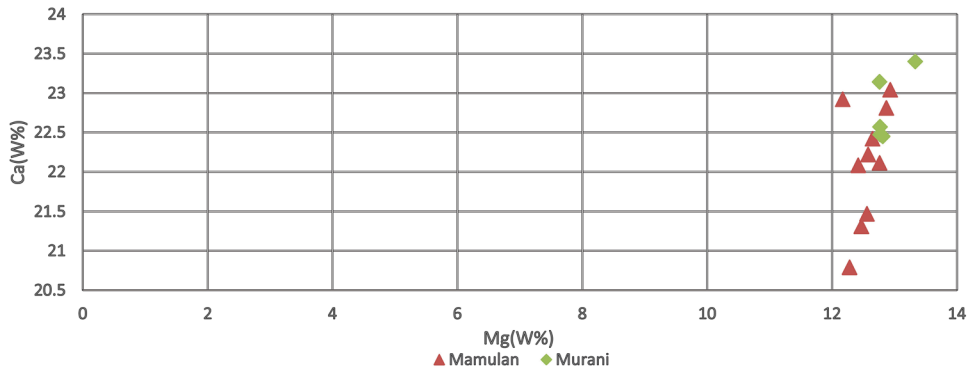

Fig. 11 Cross-plot of Ca vs. Mg for D1 of the Shahbazan Fm

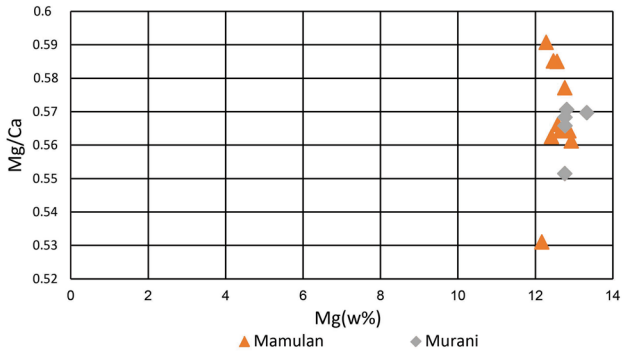

Fig. 12 Cross-plot of Mg/Ca vs. Mg, higher Mg/Ca ratio of dolomicrite (D1) in the Mamulan section and association with evaporite may imply supratidal origin for D1

also reported from mud-dominated facies and sabkha environment (Moore 1989). Relatively higher Mg/Ca content of dolomicrites of the Mamulan section is probably due to precipitation from evaporation on upper tidal flat along with evaporites (see Fig. 13, Table 4).

Some evaporitic minerals associated with typical peritidal sedimentary features are distinctive of this dolomite type. This evaporite deposits include anhydrite with 'chicken-wire' texture. (Figure 14) Lack of fauna in this microfacies suggests tidal flat depositional environment on a proximal inner ramp setting (Alsharhan et al. 2002; Rasser et al. 2005; Vaziri-Moghaddam et al. 2010; Amirshahkarami 2013). The detrital quartz content indicates proximity to terrestrial shoreline on tidal flats (Fig. 15) (Boggs 2009; Flügel 2010). Subaqueous shallow-water evaporite beds occur in marine-fed and continental setting called saltern (Warren 2016).

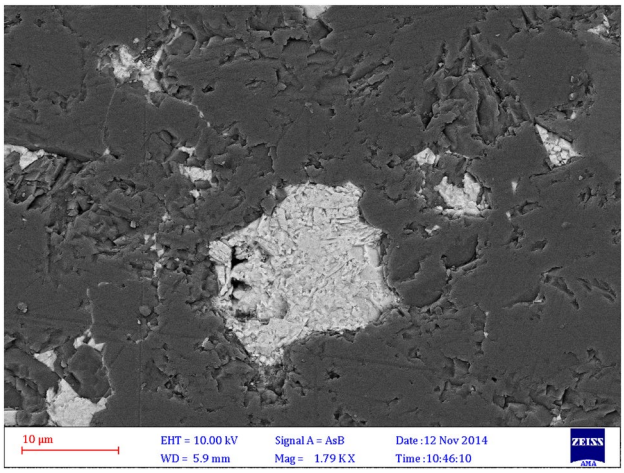

Fig. 13 SEM micrograph of evaporite (celestinobarite), Murani section; box indicates crystals which were analyzed by EDX (see Table 4)

Sr

Average Sr content of the dolomicrites is 125 and 185 ppm in D1 of the Mamulan and Murani sections, respectively (Table 1). Sr content of dolomites depends on the Sr concentration of the dolomitizing fluids. Dolomites of mixing zone have least Sr than those originated from sea water or hypersaline fluids (Land et al. 1975; Land 1985; Rao 1996). Normally, Sr content of dolomites is expected to be about 500 ppm (Tucker and Wright 1990). Therefore, low Sr content of dolomicrites of the Mamulan section are less than the expected ratio, probably due to recrystallization during later diagenesis (Veizer 1983; Azmy et al. 2011). Whereas higher Sr content of the Murani section may reflects more saline water from which they were originated (Fig. 16). The Sr content of the Tertiary marine dolomites decrease as their stoichiometry increase (Vahrenkamp and Swart 1990). It seems that stoichiometry of dolomicrites improved while their Sr decreased during diagenesis. D1 of the Mamulan

Table 4 Result of EDX analysis evaporite (celestinobarite) from Mamulan section

Elements	Ca	Ba	O	S	Sr
S (Wt%)	0.7	58.4	17	15.7	8.2

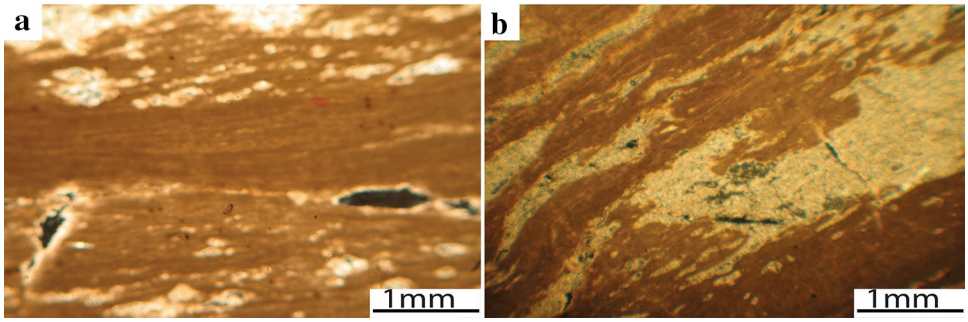

Fig. 14 **a**, **b** Photomicrographs of chicken wire texture and bedded anhydrite (Mamulan section, XPL)

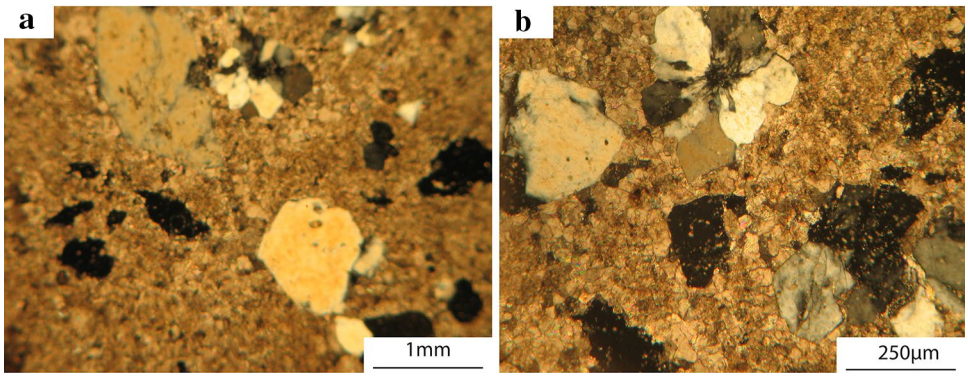

Fig. 15 **a**, **b** Quartz content associated by evaporites suggests this primary evaporite were deposited in tidal flat

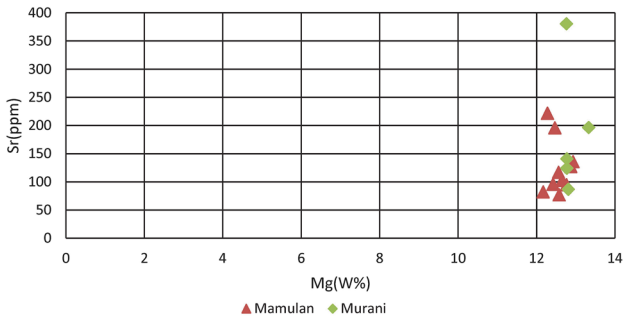

Fig. 16 Cross-plot of Sr vs. Mg for D1, Sr value depleted in those samples which experienced recrystallization, while their Mg content remains relatively constant

and Murani sections displays more stoichiometry in comparison to dolomicrites of the Shahbazan Fm. reported by Adabi (2009) and Modarress (2009) from Kialo and Darabi sections (Fig. 17). Ancient dolomites with higher Sr content are believed to originate from hypersaline fluids (Warren 1999). High water/rock ratio in open system could effectively reduce Sr/Ca ratio and increase Mn content of dolomites, whereas in closed and semi-closed systems, the Sr/Ca ratio will not change considerably in comparison to original precursors (Brand and Veizer 1981).

Evidently, a relatively closed to semi-closed diagenetic system is purposed for dolomicrites of the Shahbazan Fm. as is deduced from Fig. 18.

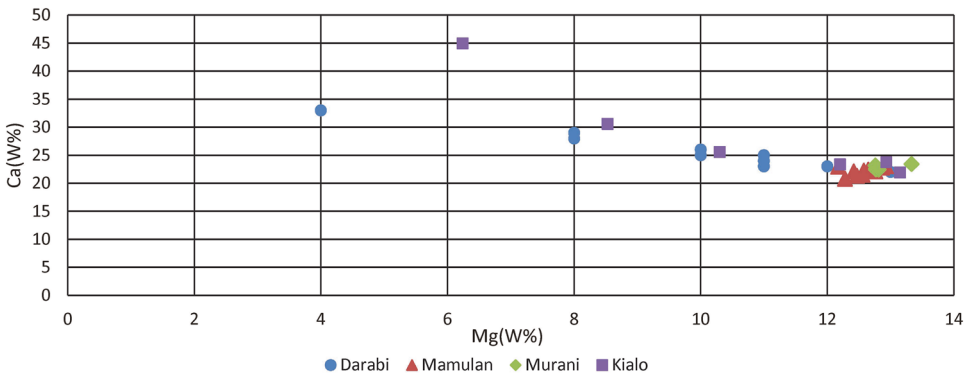

Fig. 17 Cross-plot of Ca vs. Mg. All samples of the present study suggest better stoichiometry; data labeled by circle and square are after Abdi and Adabi 2009; Modarress (2009) from Kialo and Darabi sections)

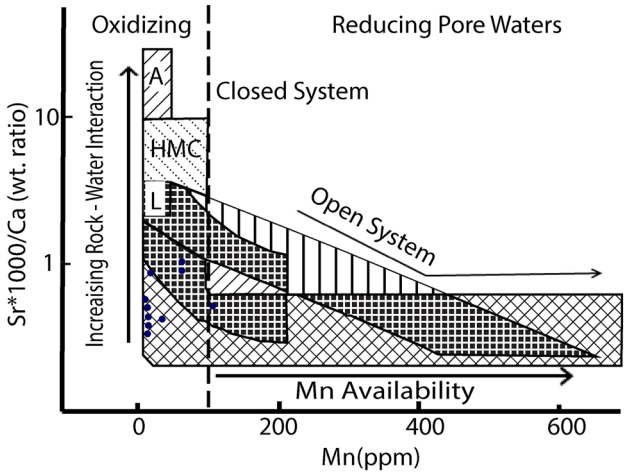

Fig. 18 Cross-plot of Mn vs. Sr/Ca (after Brand and Veizer 1980) for Mamulan section in which a closed to semi-closed system is evident

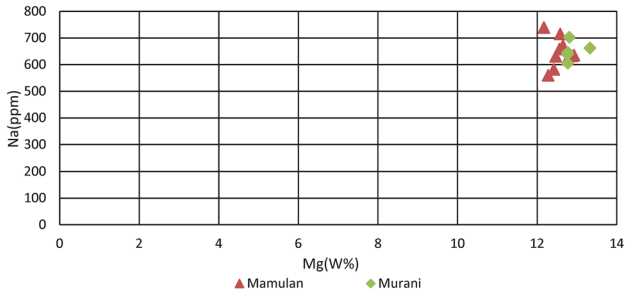

Fig. 19 Cross-plot of Na vs. Mg. Relatively elevated Na content of D_1 implies hypersaline dolomitizing fluid

Na

Average Na content of D1 is 644 and 650 ppm in Mamulan and Murani sections, respectively (Fig. 19 and Table 2). Na-rich dolomite may own their Na to saline fluid inclusions, replacement of Na ions in crystal lattice and contamination by clay minerals (Land 1980; Akçay et al. 2003; Suzuki et al. 2006; Kirmaci 2008). Na is more mobile than Sr during diagenesis of carbonate rocks (Veizer 1983). Na content of dolomicrites of the Shahbazan Fm. decreases as their Mg increase (Fig. 19). Na content of dolomicrites which originate from normal marine water is expected to vary between 110 and 160 ppm (Veizer 1983). Saline water during burial diagenesis could create Na-rich dolomite (Akçay et al. 2003; Kirmaci and Akdag 2005). However, a semi-closed to relatively closed system suggested for the study area (see Fig. 18). On the other hand, these dolomites are associated with clay minerals, with high Na content (Fig. 20). An explanation for Na content of dolomites invokes saline dolomitizing fluids (Budd 1997). Reasonably, these Na-rich dolomicrites may reflect the effect of salt water originated after reaction of fluids with evaporitic layers of the Gachsaran Fm., which overly the Asmari Fm. Furthermore, reaction with the thoroughly evaporitic Kalhur Member of the Asmari Fm. is also possible. The Kalhur Member was exclusively reported from the Asmari Fm. in the Lorestan subzone (Motiei 1995). Predominating lagoonal facies in the Murani section suggests an evaporitic condition. As well as some clay mineral content of these dolomicrites (Fig. 21, Table 5) could explain their higher Na content.

Fe and Mn

Average Fe content of the dolomicrites is 1291 and 185 ppm in Mamulan and Murani sections, respectively. Their Mn content is also 23 and less than 4 ppm, respectively. High Fe and Mn concentration suggests reaction of dolomites with reducing fluids during burial diagenesis (Dix 1993; Kirmaci 2008) (Figs. 22, 23). As the K_D (distribution coefficient) of Fe and Mn for dolomite is > 1, these elements should preferentially concentrate in the dolomites during diagenesis. However, low values (3–50 ppm for Fe and 1 ppm for Mn) reflect marine origin for dolomite, Veizer (1983); Tucker and Wright (1990). The observed low Mn content of the studied samples may reflect high rate of precipitation (Mucci 1988).

Dolomicrites comprise an average of 27.5 wt% Ca and 17.8 wt% Mg. D1 is associated with quartz and evaporite minerals (e.g., anhydrite, gypsum, celestite, and barite). Modern biotic carbonates (Arag., HMC, and LMC) have relatively higher Sr content. Selective dissolution of aragonite could supply sufficient Sr ions which is necessary for precipitation of celestite (Fig. 13, Table 4). Excess Ca ions were incorporated into the evaporitic minerals, which is probably responsible for drop in Ca content of D1 dolomite. Average Sr content of celestite is 73.22 wt%. In relatively closed system, Sr released during recrystallization of unstable carbonate minerals could reprecipitate as celestite with high Sr (Fig. 24), Yan et al. 2013).

Dolomicrosparite could generate after replacement of lime mudstone or recrystallization of dolomicrites (Al-Aasm, Packard 2000). These dolomites are also associated with peritidal sedimentary features (e.g., Lasemi et al. 2012), whereby we interpreted them as new generation after recrystallization of D1 precursors (Wierzbicki et al. 2006).

Figure 25a, b displays photomicrograph and CL microscopy of pore-filling dolomite of the Shahbazan Fm. from Murani section. Various zonations are clearly distinguishable in the CL photo (labeled through 1–6). No. 1 designates dolomicrites which were formed in oxidized

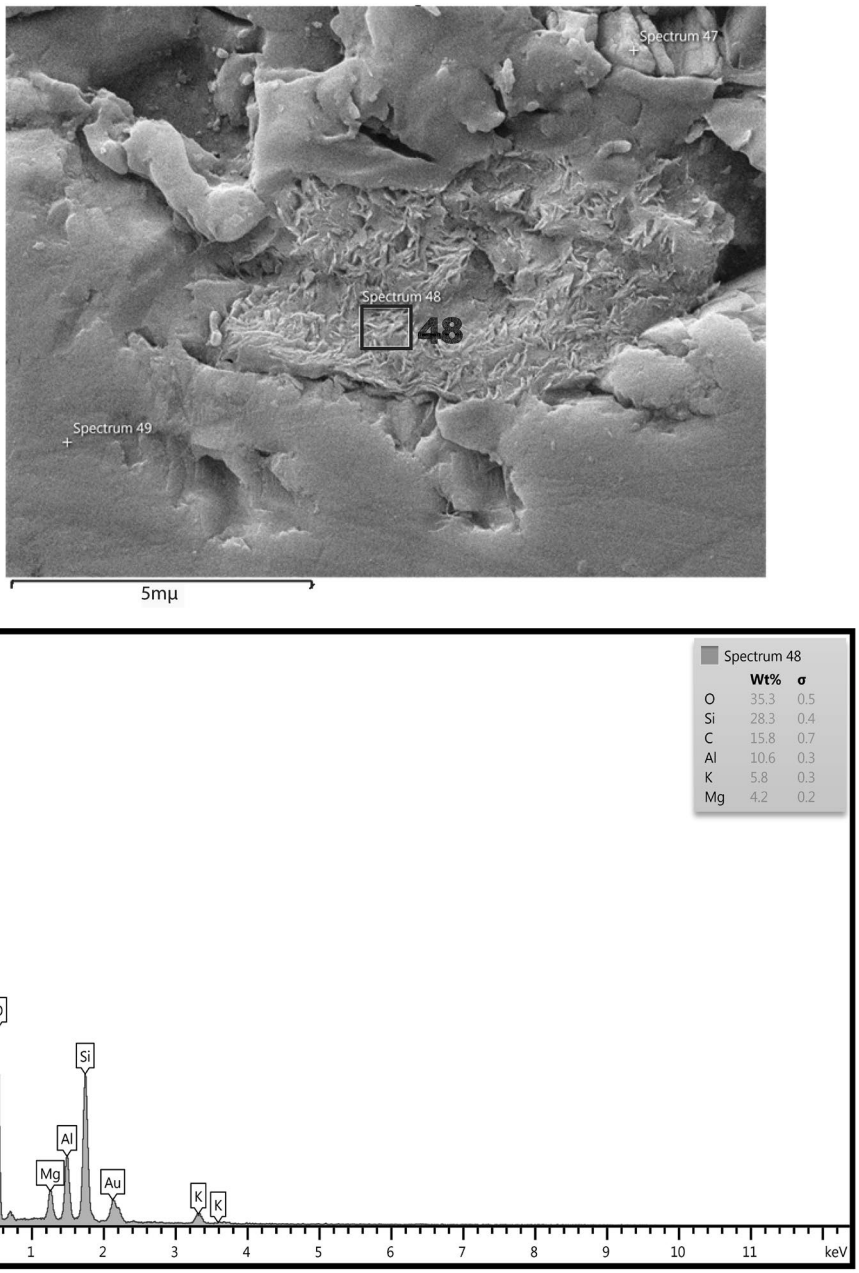

Fig. 20 SEM photograph of D1 associated with clay mineral. Point for EDX analysis and its relevant spectrum are indicated by quadrangle

eogenesis. No. 2 which is dark may imply slight effects of meteoric fluids. The rest parts show progressive increase in luminescence which is probably due to more Mn available during shallow burial (Götze 2012). However, the last one (No. 6) shows less luminescence that could be due to incorporation of some Fe into crystal lattice (Götte and Richter 2009). Such concentric zoning are assumed to be formed in a consecutive order centripetally (Wallace et al. 1991).

During flooding events (sea-level rise), fluids with different salinities could meet and subsequently mixed together, which promote limpid dolomite formation (McKenzie et al. 1980). Limpid dolomite may associate salt pseudomorphs (Folk and Siedlecka 1974; Weaver 1976; Naiman et al. 1983). As D3 sometimes concentrates around salt crystals, it probably originates during intermittent flooding events on evaporative flats. Thus, the most important diagenetic phenomenon in this formation are dolomitization, dedolomitization, and dissolution. Although calcite cements as, equant, blocky, drusy calcite, as well as dolomite cement and evaporites occluded fractures (Fig. 26, Table 3).

Although this type of dolomite does not frequently occur (< 5%), but D4 occludes any available open spaces including fractures. Non-mimic dolomitization of D4, thoroughly obliterated original sedimentary structures,

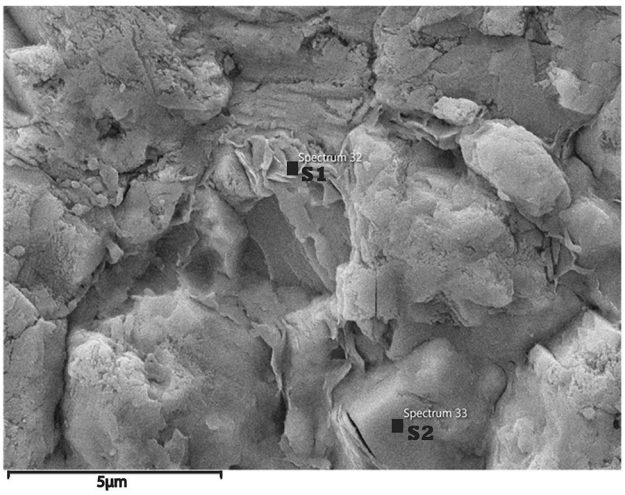

Fig. 21 SEM photo of D_4 dolomite (pore lining), diagenetic clay mineral coating on dolomite crystals is visible (S1). S1 and S2 (box) show point for EDX analysis (see Table 5), Murani section

although some vague ghosts of allochems are visible under the microscope.

Dolosparite (D5) is large crystal occluding porosities. Sibley and Gregg (1987) discussed that this dolomite could reflect slow crystal growth rate, under continuous flow of dolomitizing fluids at low temperature. Hence, D5 is interpreted to be a replacive diagenetic products of limestone precursor and/or recrystallization or D1 below CRT (critical roughening temperature (e.g., < 60 °C) (Gregg and Shelton 1990; Mazzullo 1992).

Conclusions

Based on petrography five types of dolomites were recognized within the Shahbazan Fm, namely:

- D1 (finely crystalline dolomicrites) which comprises about 90% of dolostones of the Shahbazan Fm. D1 is associated with intraclasts, algal laminite, peloids, rare bioclasts, and evaporitic minerals. D2 (dolomicrosparite) is also associated with algal laminites. D3 (limpid dolomite) is associated with evaporites such as anhydrite. D4 (pore-filling dolomite) preferentially fills pore spaces, particularly biomoldic porosity. This type is also very rare and only observed in the Murani sec-

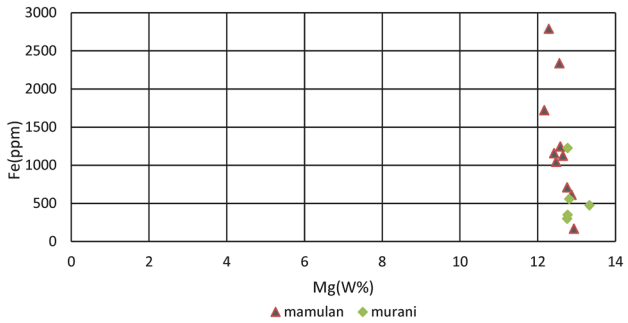

Fig. 22 Cross-plot of Fe vs. Mg. Increase in Fe content of the samples is probably due to later reaction with reducing diagenetic pore water

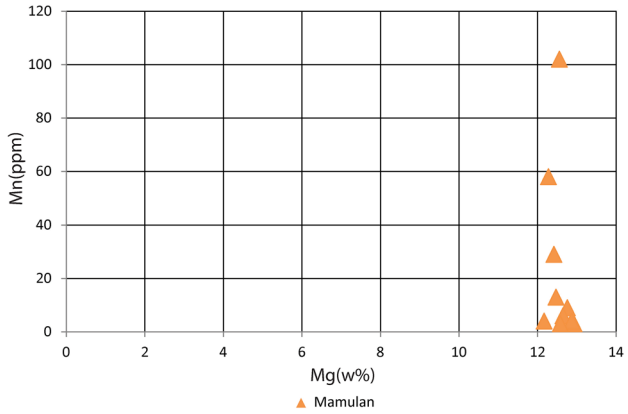

Fig. 23 Cross-plot of Mn vs. Mg. High Mn content indicates reducing conditions

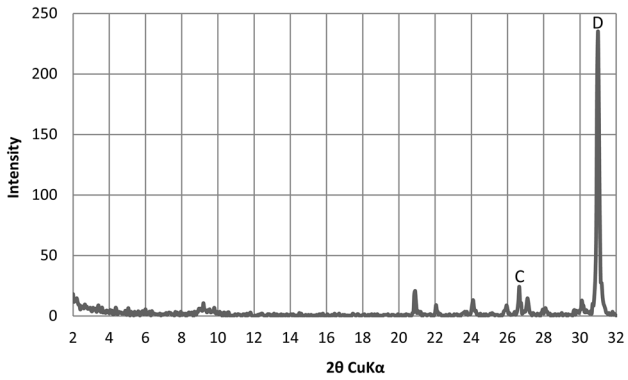

Fig. 24 An XRD graph of D1 in which occurrence of celestite is visible. *D* dolomite, *C* celestite

Table 5 Result of EDX analysis of diagenetic clay minerals in Murani section

Elements	Ca	Al	O	C	Si	Mg	K
S1 (Wt%)	2.5	6	41.1	16.4	25.1	8	0.8
S2 (Wt%)	36.8	–	30.5	15.8	–	17	–

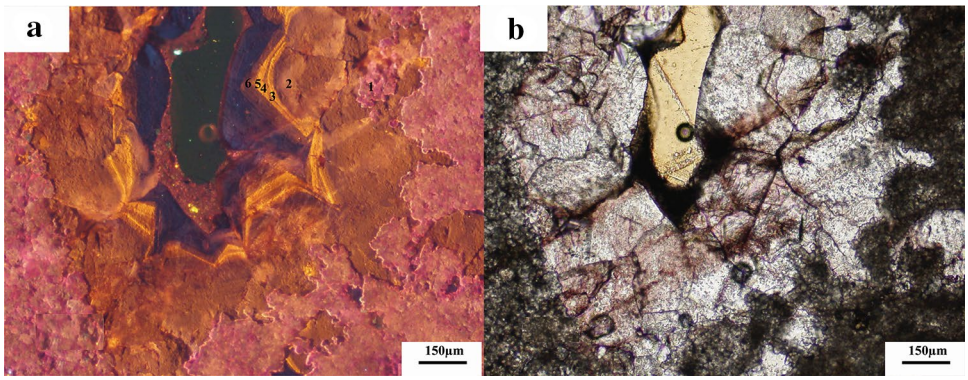

Fig. 25 CL microscopy (**a**) and photo micrograph (**b**, PPL) of pore-filling dolomite of the Shahbazan Fm. from Murani section

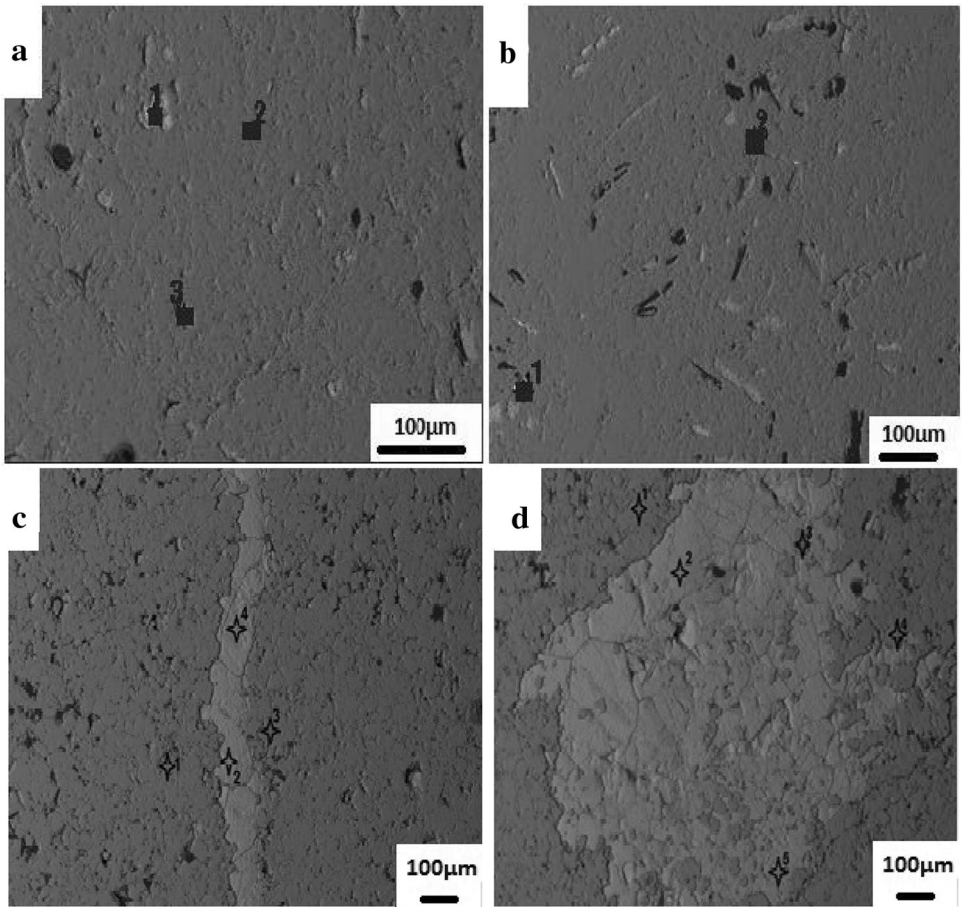

Fig. 26 Backscattered SEM image of dolomicrites, selected points for microprobe analysis (Table 3) fracture-filled calcite in dolomicrite (**a**), dedolomitization (**b**) Murani section (sample no. MS103-**a**, **b**), and backscattered SEM image of D_1 points for microprobe analysis (see Table 3) Mamulan section (sample no. MA117-**c**, **d**)

tion. D5 (dolosparite) is rare and exclusively observed only in the Murani section.

- High Mg/Ca ratio of D1 may reflect precipitation in evaporitic condition in upper intertidal setting.
- High Na may reflect saline dolomitizing fluid.
- Possibly the D1 experienced recrystallization during diagenesis, during which their Fe and Mn contents increased.

Acknowledgements Logistic and analytical costs of this research were funded by a grant to H. Mohseni via the Vice President Research Affair of the Bu-Ali Sina University. Microprobe analysis was carried out at the Geology division of Earth and Environmental Sciences of KU Leuven (Belgium). Valuable comments and help by J. Götze (Tübingen University) and G. M. Shabestary (University of Birjand) for interpretations of CL images are greatly acknowledged. Critical review and constructive comments by anonymous reviewers improved the quality of the manuscript.

References

Adabi MH (2009) Multistage dolomitization of upper jurassic mozduran formation, Kopet-Dagh Basin, n.e. Iran. Carbonates Evaporites 24(1):16–32

Abdi A, Adabi MH (2009) Dolomites petrography diagenesis analysis, probable Shahbazn-Asmari formations boundary and facies based on dolomicrite geochemistry, petrographic evidences and statistic methods in Darabi Section (Southwest Iran). Stratig Sedimentol Res 25(1):81–100 (**in Persian with abstract in English**)

Adabi MH, Rao CP (1991) Petrographic and geochemical evidence for original aragonitic mineralogy of Upper Jurassic carbonate (Mozduran Formation), Sarakhs area, Iran. Sediment Geol 72:253–267

Akçay M, Özkan HM, Spiro B, Wilson R, Hoskin PO (2003) Geochemistry of a high-T hydrothermal dolostone from the Emirili Lodemis, western Turkey, Sb-Au deposit mineral. Mineral Mag 67:671–688

Ala MA (1982) Chronology of trap formation and migration of hydrocarbons in Zagros sector, Southwest Iran. AAPG Bull 66(10):1535–1541

Ala MA, Kinghorn RRF, Rahman M (1980) Organic geochemistry and source rock characteristics of the Zagros petroleum province, Southwest Iran. J Pet Geol (JPG) 3(1):61–89

Al-Aasm IS, Packard JJ (2000) Stabilization of early-formed dolomite: a tale of divergence from two Mississippian dolomites. Sediment Geol 131:97–108

Alavi M (2004) Regional stratigraphy of the Zagros fold-thrust belt of Iran and its proforland evolution. Am J Sci 304:1–20

Alavi M (2007) Structures of the Zagros fold-thrust belt in Iran. Am J Sci 307(9):1064–1095. https://doi.org/10.2475/09.2007.02

Alsharhan AS, Kendall CG, St C (2002) Holocene carbonate/evaporites of Abu Dhabi, and their Jurassic ancient analogues. In: Barth HJ, Bore BB (eds) Sabkha ecosystems. Kluwer Academic Publisher, Netherlands, pp 187–202

Amirshahkarami M (2013) Revision in the paleontology and distribution of the larger benthic foraminifera in the Oligocene-Miocene deposits of the Zagros Basin, southwest Iran. Hist Biol 25:339–361

Azmy K, Knight I, Lavoie D, Chi G (2009) Origin of dolomites in the boat harbour formation, St. George Group, in Western Newfoundland, Canada: implications for porosity development. Bull Can Pet Geol 57:81–104

Azmy K, Brand U, Sylvester P, Gleeson SA, Logan A, Bitner MA (2011) Biogenic and abiogenic low-Mg calcite (bLMC and aLMC): evaluation of seawater-REE composition, water masses and carbonate diagenesis. Chem Geol 280:180–190

Azomani E, Azmy K, Blamey N, Brand U, Al-Aasm I (2013) Origin of lower Ordovician dolomites in eastern Laurentia: controls on porosity and implications from geochemistry. Mar Pet Geol 40:99–114

Boggs S Jr (2009) Petrology of sedimentary rocks, 2nd edn. Cambridge University Press, New York, p 600

Bordenave ML, Burwood R (1990) Source rock distribution and maturation in the Zagros orogenic belt; provenance of the Asmari and Bangestan Reservoir oil Accumulations. Org Geochem 16(1–3):369–378

Brand U, Veizer J (1980) Chemical diagenesis of a multicomponent carbonate system-1. Trace elements. J Sediment Pet 50:1219–1236

Brand U, Veizer J (1981) Chemical diagenesis of a multicomponent carbonate system-2: stable isotopes. J Sed Petr 50:987–997

Budd DA (1997) Cenezoic dolomites of carbonate Islands: their attributes and origin. Earth - Sci. Rev. 42:1–47

Choquette PW, Pray LC (1970) Geologic nomenclature and classification of porosity in sedimentary carbonates. AAPG Bull 54:207–250

Dickson JAD (1965) A modified staining technique for carbonates in thin section. Nature 205:587

Dix GR (1993) Patterns of burial and tectonically controlled dolomitization in an upper Devonian fringing—reef complex—Leduc Formation, Peace River Arch area, Alberta, Canada. J Sediment Petrol 63:628–640

Dunham RJ (1962) Classification of carbonate rocks according to depositional texture. Am Assoc Petrol Geol Memoir 1:108–121

Flügel E (2010) Microfacies of carbonate rocks: analysis, interpretation and application. Springer-Verlag, Berlin, p 976

Folk RL, Siedlecka A (1974) The schizohaline environment: its sedimentary and diagenetic fabrics as exemplified by late Paleozoic rock of Bear Island. Sediment Geol 11:1–15

Friedman GM (1965) Terminology of crystallization texture and fabric in sedimentary rocks. J Sediment Petrol 35:643–655

Götte TH, Richter K (2009) Quantitative aspects of Mn-activated cathodoluminescence of natural and synthetic aragonite. Sedimentology 56:483–492

Götze J (2012) Application of cathodoluminescence microscopy and spectroscopy in geosciences. Microsc Microanal 18:1270–1284

Gregg JM, Shelton KL (1990) Dolomitization and neomorphism in the backreef facies of the Bonneterre and Davies Formations (Cambrian), southeastern Missouri. J Sediment Petrol 60:549–562

Gregg JM, Sibley DF (1984) Epigenetic dolomitization and the origin of xenotopic dolomite texture reply. J Sedimen Petrol 56:735–763

Haeri Ardakani O, Al-Aasm I, Coniglio M, Simon I (2013) Diagenetic evolution and associated mineralization in middle Devonian carbonates, southwestern Ontario, Canada. Bull Can Pet Geol 61(1):41–68

Heydari E (2008) Tectonics versus eustatic control on supersequences of the Zagros Mountains of Iran. Tectonophysics 451:56–70

James GA, Wynd JG (1965) Stratigraphic nomenclature of Iranian oil consortium agreement area. Am Assoc Pet Geol Bull 49(12):2182–2245

Kaczmarek SE, Sibley DF (2011) On the evolution of dolomite stoichiometry and cation order during high-temperature synthesis experiments: an alternative model for the geochemical evolution of natural dolomites. J Sediment Geol 240:1–11

Kirmaci MZ (2008) Dolomitization of the late Cretaceous—Paleocene platform carbonates, Golkoy (Ordu), eastern Pontides, NE Turkey. J Sediment Geol 203:289–306

Kirmaci MZ, Akdag K (2005) Origin of dolomite in the late cretaceous Paleocene limestone turbidites, Eastern Pontides, Turkey. J Sediment Geol 181:39–57

Land LS (1980) The isotopic and trace element geochemistry of dolomite, concepts and models of dolomitization. SEPM Spec Publ 28:87–110

Land LS (1985) The origin of massive dolomite. J Geol Educ 33:112–125

Land LS, Lang J, Smith VN (1975) Preliminary observations on the carbon isotopic composition of some reef coral tissue and symbiotic zooxanthellae. Limnol Oceanogr 20(2):283–287

Lasemi Y, Jahani D, Amin-Rasouli H, Lasemi Z (2012) Ancient Carbonate Tidalites. In: Davis RA Jr, Dalrymple RW (eds) Principles of tidal sedimentology. Springer Science + Business Media, Berlin, pp 567–606

Machel HG (2000) Dolomite formation Caribbean islands-driven by plate tectonics? J Sediment Res 70:977–984

Mazzullo SJ (1992) Geochemical and neomorphism alteration of dolomite: a review. Carbonate Evaporite 7:21–37

McKenzie JA, Hsu K, Schneider JF (1980) Movement of subsurface waters under the sabkha, Abu Dhabi, UAE, and it's relation to evaporative dolomite genesis. In: Zenger DH, Dunham JB,

Ethington RL (eds) Concepts and models of dolomitization, 28th edn. SEPM Spec. Publ., Tulsa, pp 11–30
Modarress MH, Adabi MH (2009) Dolomitization of Shahbazan Formation at Kialu section. 27th IAS meeting
Mohseni H, Abdollahpour M, Rafiei B, Mohsenipour F (2012) Geochemistry of carbonate formations in southwestern Kermanshah Province, emphasize on the role of dolomitization on karst enhancement. Proceeding of the 29th IAS Meeting of Sedimentology, Schladming, Austria
Mohseni H, Al-Aasm IS (2004) Tempestite deposits from a storm influenced carbonate ramp: an example from the Pabdeh formation, Zagros Basin, SW Iran. JPG 27(2):163–178
Mohseni H, Behbahani R, Khodabakhsh S, Atashmard Z (2011) Depositional environments and trace fossil assemblages in the Pabdeh Formation (Paleogene), Zagros Basin, Iran. N Jb Geol Paläont Abh 262(1):59–77
Mohseni H, Hassanvand V, Homaei M (2016) Microfacies analysis, depositional environment and diagenesis of the Asmari-Jahrum reservoir in Gulkhari oil field, Zagros basin, SW Iran. Arab J Geosci 9:113. https://doi.org/10.1007/s12517-015-2130-y
Moore CH (1989) Carbonate diagenesis and porosity. Elsevier, Amsterdam, p 338
Motiei H (1995) Petroleum geology of the Zagros, Treatise in geology of Iran (two vol. in Persian), Geol Survey of Iran. p 1009 (in Persian)
Mucci A (1988) Manganese uptake during calcite precipitation from seawater: conditions leading to the formation of a pseudokutnahorite. Geochim et Cosmochim Acta 52(7):1859–1868
Murris RJ (1980) Middle east: stratigraphic evolution and oil habitat. AAPG Bull 64(5):597–618
Naiman ER, Bein A, Folk RL (1983) Complex polyhedral crystals of limpid dolomite associated with halite, Permian upper clear Fork and Glorieta Formation, Texas. JSP 53(2):549–555
Rao CP (1996) Modern carbonates tropical, temperate, polar: introduction to sedimentology and geochemistry. Arts of Tasmania, Tasmania, p 206
Rasser MW, Scheibner C, Mutti M (2005) A paleoenvironmental standard section for Early Ilerdian tropical carbonate factories (Corbieres, France; Pyrenees, Spain). Facies 51(1):217–232
Razin P, Taati F, van Buchem FSP (2010) An outcrop reference model for the Arabian Plate non-marine deposits. Earth Sci Rev 98:217–268
Sass E, Bein A (1988) Dolomites and salinity, a comparative geochemical study. In: Shukla V, Baker PA, (eds) 1988. Sedimentology and spec, 43 edn. p 223–233
Sepehr M, Cosgrove JW (2004) Structural framework of the Zagros Fold-Thrust Belt, Iran. Mar Pet Geol 21:829–843
Sibley DF, Gregg JM (1987) Classification of dolomite rocks textures. J Sediment Petrol 57:967–975
Stocklin J (1968) Structural history and tectonics of Iran: a review. AAPG Bulletin 52:1229–1258
Suzuki Y, Iryu Y, Inagaki S, Yamada T, Aizawa S, Budd DA (2006) Origin of atoll dolomites distinguished by geochemistry and crystal chemistry: Kita-daito-jima, northern Philippine Sea. Sediment Geol 183:181–202
Tucker ME, Wright VP (1990) Carbonate Sedimentology. Blackwell Scientific Publications, Oxford, p 482
Vahrenkamp VC, Swart PK (1990) New distribution coefficient for the incorporation of strontium into dolomite and its implications for the formation of ancient dolomites. Geology 18(5):387–391
Vaziri-Moghaddam H, Seyrafian A, Taheri A, Motiei H (2010) Oligocene-Miocene ramp system (Asmari Formation) in the NW of the Zagros basin, Iran: microfacies, paleoenvironment and depositional sequence. Rev Mexicana Cien Geol 27:56–71
Veizer J (1983) Chemical diagenesis of carbonates: theory and application of trace element technique. Stable Isotopes Sediment Geol 10:3–100
Warren JK (1999) Evaporites: their evolution and economics. Blackwell Scientific Publications, Oxford, p 438
Warren JK (2000) Dolomite: occurrence, evolution and economically important association. Earth Sci Rev 52:1–81
Warren J (2016) Evaporites: sediments, resources and hydrocarbons, 2nd edn. Springer-Verlag, Berlin Heidelberg, p 1813
Weaver CE (1976) Construction of limpid dolomite. Geology 4:425–428
Wierzbicki R, Dravis JJ, Al-Aasm I, Harland H (2006) Burial dolomitization and dissolution of upper Jurassic Abenaki platform carbonates, Deep Panuke reservoir, Nova Scotia, Canada. AAPG Bull 90(11):1843–1861
Yan H, Shao D, Wang Y, Sun L (2013) Sr/Ca profile of long-lived Tridacna gigas bivalves from South China Sea: a new high-resolution SST proxy. Geochim Cosmochim Acta 112:52–65